

## Article

# Characteristics of Heat Waves in Mainland China since 1961 Based on Absolute and Relative Methods

Honghua Ji <sup>1</sup>, Aiqing Feng <sup>2</sup>, Yufei Zhao <sup>3</sup>, Jie Liao <sup>3</sup>, Zhisen Zhang <sup>3</sup>, Changgui Gu <sup>1</sup> and Aixia Feng <sup>3,\*</sup>

<sup>1</sup> Department of Systems Science, Business School, University of Science and Technology, Shanghai 200093, China; 212150973@st.usst.edu.cn (H.J.); guchanggui@usst.edu.cn (C.G.)

<sup>2</sup> National Climate Center CMA, Beijing 100081, China; fengaq@cma.gov.cn

<sup>3</sup> National Meteorological Information Center CMA, Beijing 100081, China; zhaoyf@cma.gov.cn (Y.Z.); liaoj@cma.gov.cn (J.L.); zhangzs@cma.gov.cn (Z.Z.)

\* Correspondence: fengax@cma.gov.cn

**Abstract:** Based on gridded temperature data from the China Meteorological Administration (CMA), two types of methods, i.e., absolute methods and relative methods, respectively, were used to identify heat waves in Mainland China. Four statistical indicators, including the occurrence frequency, duration days, earliest occurrence date, and latest extinction date, were constructed to analyze the spatial-temporal characteristics of heat waves, especially on the annual and decadal change trends. Firstly, we found that both the frequency and the duration of heat waves decreased in the period from 1960 to 1989 but increased in the 1990s and increased significantly from the early 2000s to the 2010s. Spatially, the frequency and the duration obtained by each type of method are significantly different among different regions when considering different facts, such as different regions that have different degrees of tolerance to heat waves. Secondly, the decadal distribution characteristics of the earliest occurrence date and the latest extinction date of heat waves well capture the hot summer, the stronger sensitivity of winter to warming than other seasons, and the gradually increasing intensity of heat waves. It provides a multidimensional reference for the cause analysis and prediction of extreme heat waves in China.

**Keywords:** heat waves; spatial and temporal characteristics; evolution; China



**Citation:** Ji, H.; Feng, A.; Zhao, Y.; Liao, J.; Zhang, Z.; Gu, C.; Feng, A. Characteristics of Heat Waves in Mainland China since 1961 Based on Absolute and Relative Methods. *Atmosphere* **2023**, *14*, 544. <https://doi.org/10.3390/atmos14030544>

Academic Editor: Matthew Eastin

Received: 13 February 2023

Revised: 4 March 2023

Accepted: 8 March 2023

Published: 12 March 2023



**Copyright:** © 2023 by the authors. Licensee MDPI, Basel, Switzerland. This article is an open access article distributed under the terms and conditions of the Creative Commons Attribution (CC BY) license (<https://creativecommons.org/licenses/by/4.0/>).

## 1. Introduction

According to the Sixth Assessment Report for the United Nations Intergovernmental Panel on Climate Change (IPCC), the rate of climate warming is accelerating, and the scale of changes in the whole climate system is unprecedented in centuries or even millennia [1]. Under the background of global warming, heat waves occur frequently and intensively [2–5]. Heat waves are projected to intensify, accelerate, and increase in intensity, frequency, and duration by the end of the 21st century [6–8]. In 2003, a catastrophic heat wave occurred in Europe, which affected many local residents [9,10]. In 2010, a huge heat wave occurred in Russia [11–13]. In 2013, eastern China suffered from unprecedented heat waves for almost the whole summer [14]. In 2017, the heat wave swept Central and Western Europe [15]. Heat waves not only affect human health but also pose a major threat to the ecological environment as well as the social economy [4,16–20]. Both the human death and the economic loss caused by heat waves every year cannot be underestimated. Drought caused by persistent high temperatures has dealt a fatal blow to agriculture and animal husbandry [21]. Moreover, the frequent occurrence of heat waves has increased human mortality [22,23]. Among the extreme events, the influence of heat waves is the most extensive and expanding. With the increase in its intensity, frequency, and range, heat waves have become the focus and hot spot of scientists' research in recent years [24–27].

A heat wave is a weather process in which the temperature is higher than the long-term average climate for several consecutive days. Both the definition and the identifi-

cation methods of heat waves have not yet formed a unified criterion [28,29]. The heat wave can be defined by the daily maximum temperature, daily average temperature, daily minimum temperature, and meteorological factors related to the formation of high temperatures [30–32]. According to the setting method of the high-temperature threshold, the definition methods of heat waves can be roughly divided into two categories, which are absolute threshold methods and relative threshold methods [33]. In the following, we provide some absolute methods. The World Meteorological Organization (WMO) proposes the definition of a heat wave as a process in which the daily maximum temperature is higher than 32 °C and lasts for 3 days or more [34]. The Royal Netherlands Meteorological Institute defines a heat wave as a weather process in which the daily maximum temperature is greater than 25 °C, the duration is greater than 5 days, and the daily maximum temperature is not lower than 30 °C for at least 3 of these 5 days [35]. China Meteorological Administration defines the operation standard of heat waves as a daily maximum temperature that is less than 35 °C and the duration of heat waves for 3 days or more [36,37]. Based on absolute methods, a great deal of research already exists. In terms of the 35 °C threshold, Tan et al. [38] screened the heat waves in Shanghai in 1998 and 2003 to explore the effect of different heat wave intensities on mortality, which described that mortality was closely related to the duration of heat waves. Li et al. [39] analyzed spatiotemporal changes in heat waves and extreme temperatures in the main cities of China from 1955 to 2014, which revealed that heat waves showed an increasing trend in most regions from 1955 to 2014, with a more obvious increasing trend after the late 1980s compared to the decades before. Meanwhile, plenty of researchers used relative methods to define the heat wave. Cowan et al. [40] took the 90th percentile of the highest temperature of a station as the discriminant threshold of heat waves in consideration of the vast territory, large differences in topography, and diverse climate of Australia, which captured the spatial distribution of the frequency and duration of summer heat waves. Ding et al. [41] used the 90th percentile of temperature sequence as the recognition threshold of heat waves to analyze the changing trend of heat waves in China and found that heat waves occurred most frequently in the northwest and southeast China. Perkins et al. [29] used the Berkeley Earth dataset to select the 90th percentile as the threshold of heat waves to analyze the frequency, duration, and variation trend of global heat waves, which was described with an obvious increase. Zimmer et al. [42] analyzed the health effects and changes in heat waves using a 5 °C threshold, and there was a statistically significant increase in emergency hospital admissions during heat waves.

In recent years, many researchers have focused on the generation and variation in heat waves in China. So far, there is a significant warming trend in China [28,42–46]. Studies revealed that the frequency and intensity of heat waves observed in China in 2018 were approximately double that of 1960 [47]. China has been one of the countries most affected by climate change due to its distinct monsoon climate [46]. Previous studies have suggested that decreasing snow cover over the western Tibetan Plateau and its association with the Mongolian high may have encouraged heat waves in northern China, while anthropogenic influences have increased the likelihood of extreme summer heat waves in eastern China [6]. Heat waves occur frequently in China and cause serious harm. Therefore, we chose a variety of heat wave identification methods to analyze the temporal and spatial characteristics of heat waves in mainland China, aiming at grasping the evolution law of heat waves from multiple perspectives so as to forecast heat waves and reduce the harm of heat waves. The spatiotemporal characteristics and evolutionary process of the four statistical features were also analyzed. The main gap between this study and the existing ones lies in the research methods. Using the relative method, this study constructs a new set from the same day in 60 years for each grid point. The heat wave threshold of each grid point for each day is calculated separately. Some studies have been conducted to construct new sets by taking different window sizes. This study pays more attention to the temperature information of the historical field and future field while existing studies pay more attention to the temperature information closer to the calendar day. In addition, we compared the

rigor and emphasis of the three relative methods for heat wave identification. In terms of statistical characteristics, this study not only analyzed the spatiotemporal characteristics and decadal changes in the frequency and intensity of heat waves but also analyzed the evolution process of the earliest occurrence date and the latest extinction date of heat waves, which drew conclusions corresponding to the facts.

Based on the temperature data of meteorological grids in China from 1961 to 2020, the absolute method and three different relative methods were used to identify heat waves in each grid, and four statistical indicators were constructed, which are the frequency of heat waves, the duration of heat waves, the earliest occurrence date of heat waves, and the latest extinction date of heat waves. The trends and spatiotemporal characteristics of the annual and decadal changes of the four statistical indicators were analyzed. The results of the absolute and relative methods were compared between groups (the absolute method vs. the relative method) and within groups (among the three relative methods) to obtain the similarities and differences among them. In this study, we used multiple methods to construct the four statistical indicators simultaneously, focusing on their spatiotemporal characteristics and evolution processes. Compared with other studies, we comprehensively considered different methods to identify heat waves and then developed different datasets to analyze the characteristics and evolution of heat waves under different methods, providing a multi-dimensional reference for the cause analysis and prediction of extreme heat events in China.

## 2. Data and Methods

### 2.1. Data

The data used in this research is the  $0.5^\circ \times 0.5^\circ$  gridded datasets of daily surface temperature in Mainland China, which is based on the basic meteorological elements data of 2472 national surface meteorological stations in China (excluding the two far-sea island stations of Xisha and Coral) and compiled by the latest basic data special project. The thin plate spline (TPS) method combined with three-dimensional geospatial information has been used for spatial interpolation to establish daily temperature grid data with  $0.5^\circ \times 0.5^\circ$  horizontal resolution in China since January 1961. In this study, the daily maximum temperature data of this dataset were selected from 3830 grids in China, and the time range was from 1 January 1961 to 31 December 2020 (a total of 60 years).

### 2.2. Methods

In this study, absolute and relative methods were used to calculate the number of heat waves. These include the duration of heat waves, the earliest date of heat wave occurrence, and the latest date of heat wave extinction. Based on these four statistical characteristics, the changing trend of heat waves in China over the past 60 years was analyzed.

#### 2.2.1. Absolute Method

In meteorological operations, a high-temperature day is usually defined as the day with the highest temperature, which can be no less than  $35^\circ\text{C}$ , and a weather process with three consecutive high-temperature days or more is defined as a heat wave [37]. The absolute method of identifying a heat wave in a single grid point is that the maximum temperature for more than three consecutive days should not be lower than  $35^\circ\text{C}$ . The absolute threshold is defined as:

$$T_{i,j}^n \geq 35 \quad (1)$$

where  $T_{i,j}^n$  represents the maximum temperature of the  $n^{\text{th}}$  grid point on the  $j^{\text{th}}$  calendar day in year  $i$ .

#### 2.2.2. Relative Methods

In this study, three different relative methods were used to calculate the heat waves in China over the past 60 years. The maximum temperature of a grid for three consecutive

days and above was not lower than the 90th percentile value of the temperature series [48], which is named the percentile threshold method (PTM). The anomaly of the daily maximum temperature at a certain grid for three consecutive days or more was no lower than 5 °C [42], which is named the fixed anomaly threshold method (FATM). The anomaly of the daily maximum temperature for three or more consecutive days at a grid point is no lower than two times the standard deviation of the historical temperature series of that day, which is named the variable anomaly threshold method (VATM).

The use of PTM or FATM to identify heat waves is well documented. The reasons for using VATM are shown below. The temperature follows the normal distribution and exists under the 2-sigma principle. The probability of the value distribution in  $(\mu - 2\sigma, \mu + 2\sigma)$  is 0.9544. Therefore, the probability of an anomaly that is greater than two standard deviations is  $(1 - 0.9544)/2 = 0.0228 < 0.05$ , which can be regarded as a small probability event, in line with the small probability characteristics of heat waves.

Considering the complexity and feasibility of the calculation, the maximum temperature data on 29 February in a leap year is not used in the calculation of anomaly and the two times standard deviation of historical temperature series in the relative method. The number of annual maximum temperature data for each grid point was unified into 365 according to the total amount of 60 years from 3830 grid points which are 83,877,000 (Figure 1).

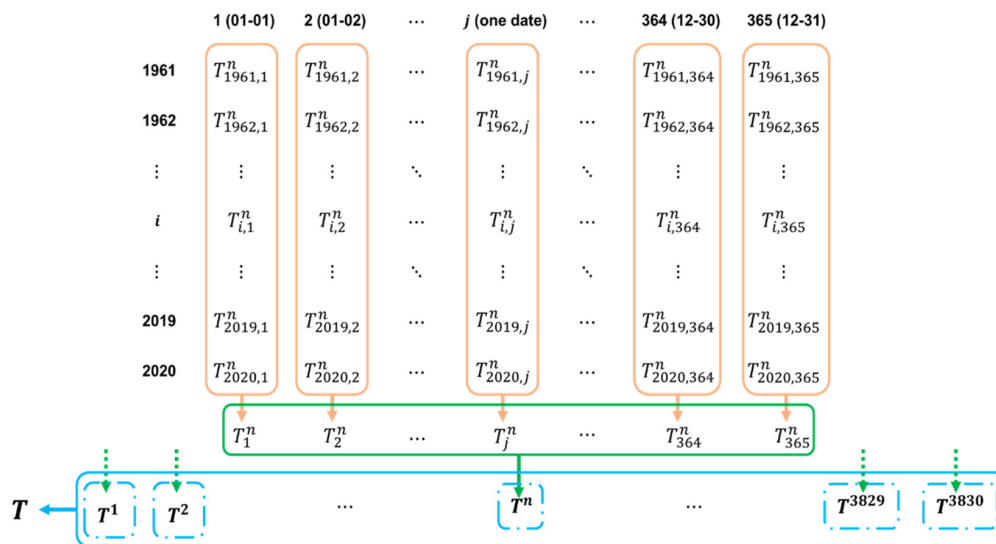


**Figure 1.** The set in the module highlighted in green is used to calculate the 90th percentile of the maximum temperature at one grid point. The set in the module highlighted in orange is used to calculate the anomaly and standard deviation of maximum temperatures at one grid point on one calendar day. It can be easily understood that we set 3830 different thresholds for PTM and  $3830 \times 365 = 1,397,950$  different thresholds for FATM or VATM.

The first, second, and third relative thresholds are defined as follows, where the 90<sup>th</sup> percentile represents the function for calculating the 90th percentile.  $T^n$  represents the set of maximum temperatures at the  $n^{\text{th}}$  grid point for 60 years. The mean represents the function for calculating the average.  $T_j^n$  represents the set maximum temperature at the  $n^{\text{th}}$  grid point on the  $j^{\text{th}}$  calendar day in each year.  $std$  is a function for calculating the standard deviation.

$$T_{i,j}^n \geq 90^{\text{th}} \text{ percentile}\{T^n\} \tag{2}$$

$$T_{i,j}^n - \text{mean}\{T_j^n\} \geq 5 \tag{3}$$

$$T_{i,j}^n - \text{mean}\{T_j^n\} \geq 2 \times \text{std}\{T_j^n\} \tag{4}$$

### 2.2.3. Locally Weighted Scatterplot Smoother

A locally weighted scatterplot smoother (LOWESS) was proposed by William [49]. Its purpose is to predict and smooth. When there are outliers in the coefficient estimates, it is necessary to ensure valid estimates and eliminate outliers by reasonable means. LOWESS can handle this easily.

The following demonstrates how LOWESS works. With a point  $(x_i, y_i)$  as the center, a data set  $Y_s = \left\{ \begin{matrix} [i+\frac{s-1}{2}] \\ \cup \\ [i-\frac{s-1}{2}] \end{matrix} y_i \right\}$  of length  $s$  is selected forward and backward. The prediction set  $\hat{Y}_s = \left\{ \begin{matrix} [i+\frac{s-1}{2}] \\ \cup \\ [i-\frac{s-1}{2}] \end{matrix} \hat{y}_i \right\}$  was obtained by weighted polynomial regression for the  $s$  data points. Calculate the central value  $(x_i, \hat{y}_c)$  of the prediction set, which satisfies  $\hat{y}_c = \max\{\hat{Y}_s\} - \frac{\max\{\hat{Y}_s\} - \min\{\hat{Y}_s\}}{2}$ . All the data points are traversed to obtain  $n$  central values, which are connected to form the LOWESS curve.

## 3. Results

### 3.1. Analysis of Temperature Change in China from 1961 to 2020

From 1961 to 2020, the mean value of the daily maximum temperature in China was first stable and then increased significantly from the 1980s, and the standard deviation of the daily maximum temperature in China first decreased and then remained unchanged. The turning point of the change in the mean is around 1980, and the turning point of the change in the standard deviation is around 1990. The rise of the mean value and the decline of the standard deviation leads to the right shift in the probability distribution function of the daily maximum temperature and a higher peak value, so the probability of an extremely high-temperature increase and the probability of low-temperature decreases (Figure 2), which corresponds to the increasing global warming and the frequent occurrence of heat waves in recent years.

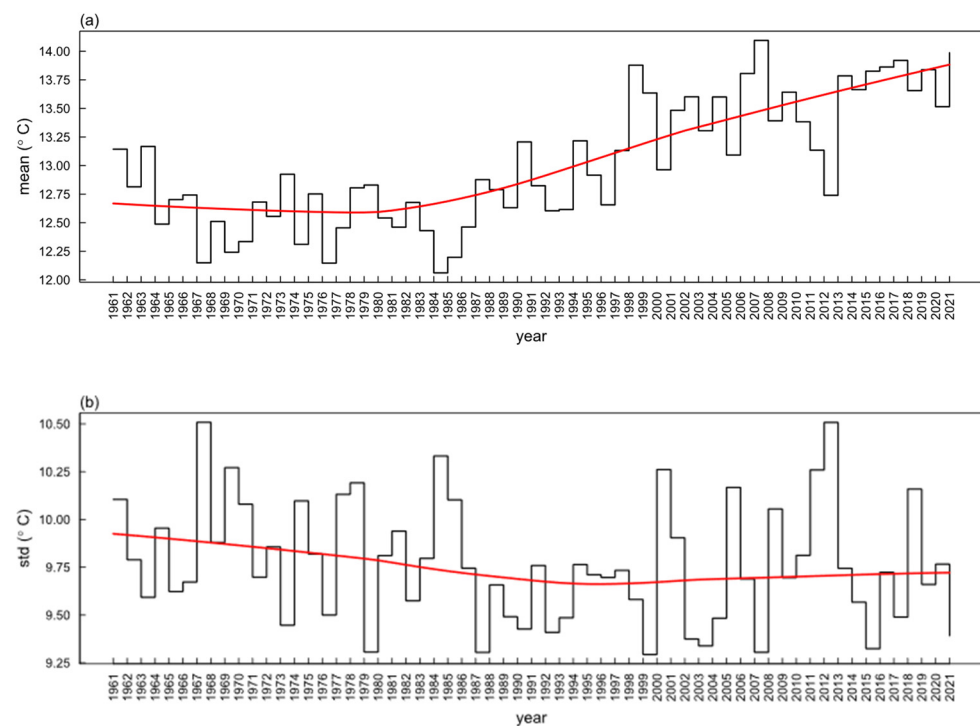


**Figure 2.** Histogram of the mean and standard deviation of the daily maximum temperature series for all grid points from 1961 to 2021 and its LOWESS trend fitting line. (a) Shows the mean of the daily maximum temperature series for all grid points from 1961 to 2021, and (b) Shows the standard deviation of the daily maximum temperature series for all grid points from 1961 to 2021.

### 3.2. Analysis of Decadal Variation of Heat Wave Characteristics in China from 1961 to 2020

In this study, the period 1961–2020 was divided into six decades, namely 1961–1970, 1971–1980, 1981–1990, 1991–2000, 2001–2010, and 2011–2020. One decade is a decadal period.

#### 3.2.1. Results Based on Absolute Method

##### (1) Frequency and Intensity

Figure 3 shows the distribution of the average occurrence times of heat wave years when screened by the absolute method. In terms of the occurrence region of heat waves, the common characteristics of the frequency of the heat wave in the six decades are as follows. The frequency of heat waves in the middle and lower reaches of the Yangtze River, Jianghuai region, and Xinjiang is significantly more than that in other regions of China. Northeast China and Inner Mongolia experience heat waves, but less frequently. Tibet and Qinghai hardly experience heat waves. In terms of spatial and temporal variations in heat waves, the frequency and spatial range of heat waves in the 1970s decreased compared with that in the 1960s and then reached the bottom in the 1980s. It began to increase in the 1990s and zoomed in frequency and spatial range after the 21st century.

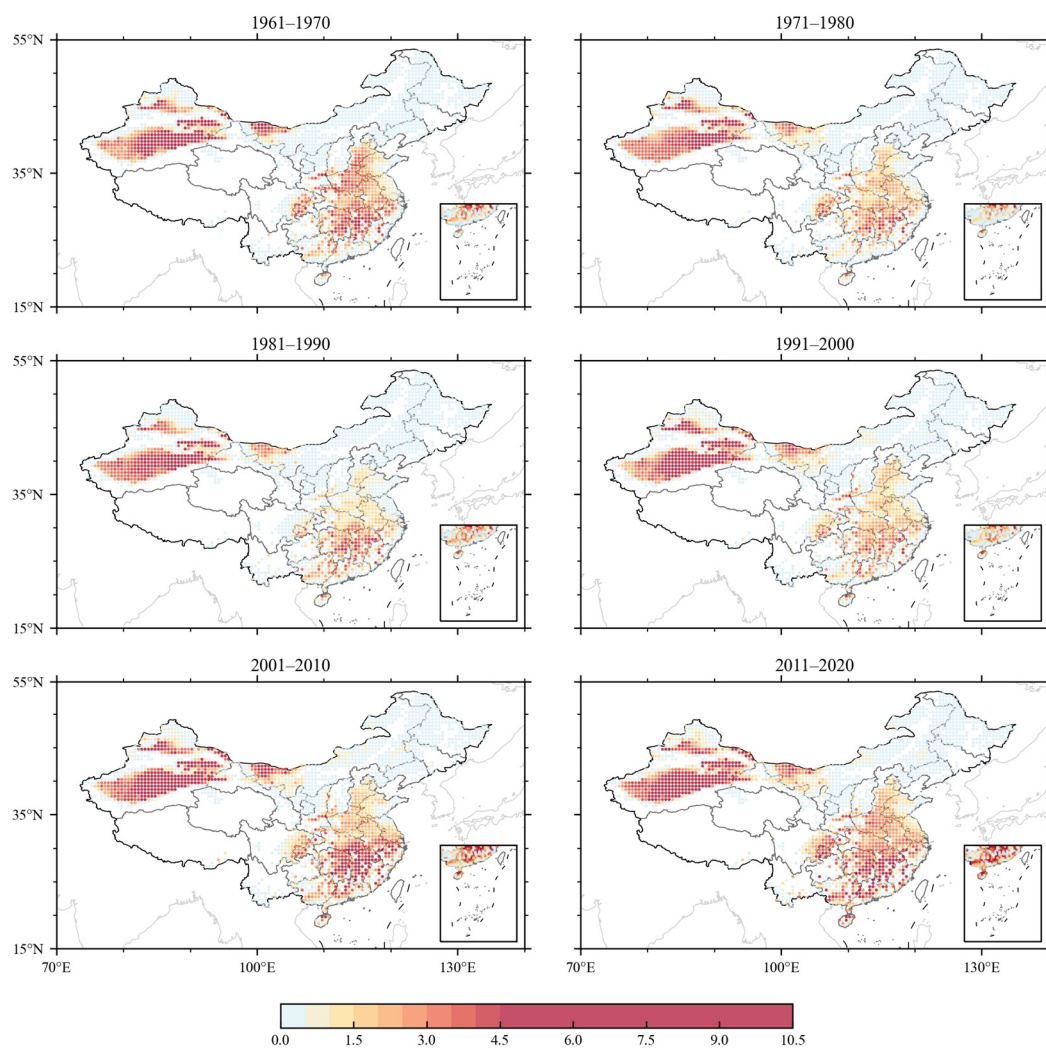


**Figure 3.** Distribution diagram of the average frequency of heat waves in each decade based on the absolute method.

The same characteristics in the intensity of heat waves over the six decades were that the duration of heat waves became longer in Xinjiang province and the middle and lower reaches of the Yangtze River, some heat waves appeared to be more prolonged, heat waves

occurred sporadically in the Jianghuai region, and the duration of heat waves in Northeast China and Inner Mongolia was basically less than 10 days (Figure 4).

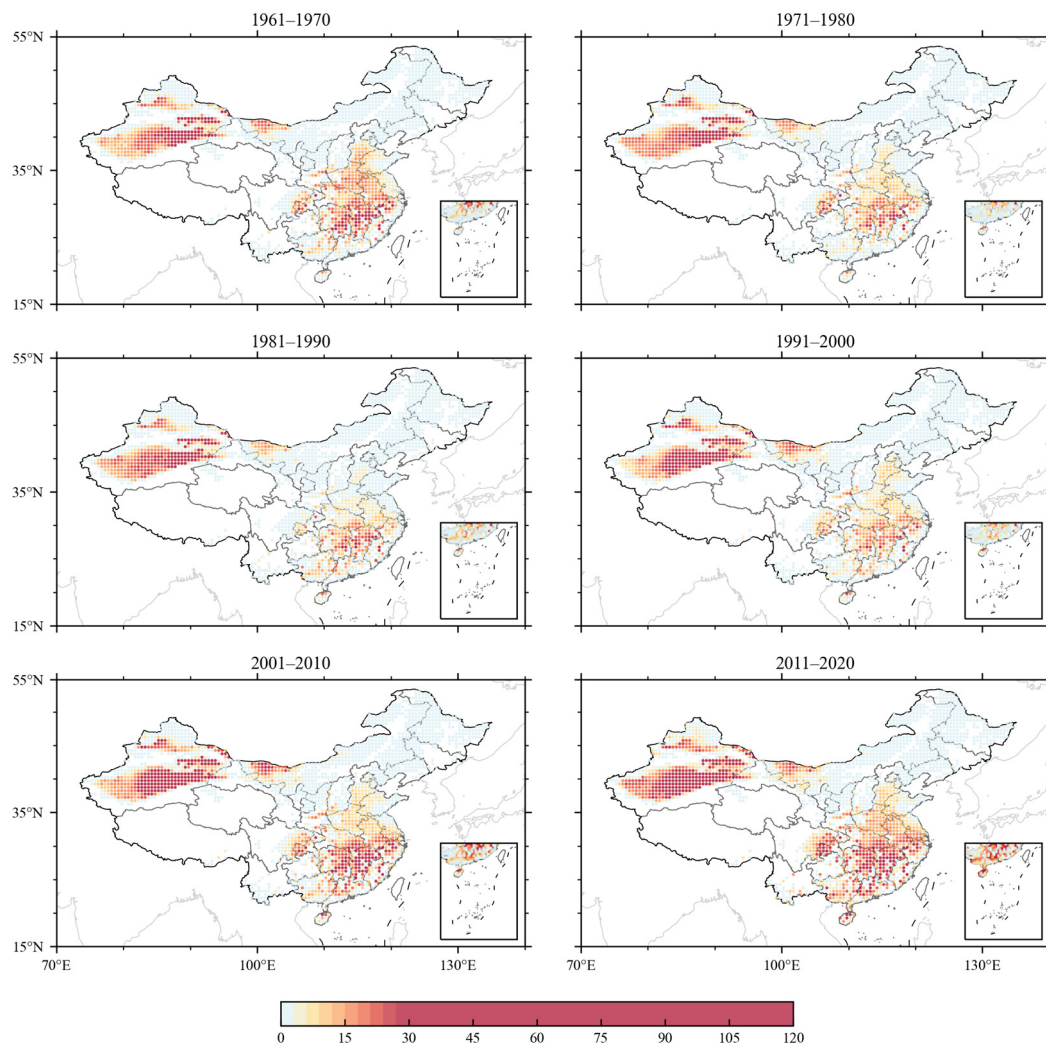


**Figure 4.** Distribution diagram of the average duration of heat waves in decadal period based on absolute method.

It can be seen from Figures 3 and 5a that the variation trend in the decadal average frequency of heat waves from 1961 to 2020 decreased first and then increased. The decrease was obvious for the average frequency of decadal heat waves in the middle and lower reaches of the Yangtze River and the Jianghuai region during 1971–1980 and 1981–1990. This also corresponded to the low mean and high standard deviation in Figure 2 from 1971 to 1990. The low mean and high standard deviation reflects the left-leaning and peak decline of the probability distribution function of the daily maximum temperature, which leads to a decrease in the probability of occurrence and the average frequency of heat waves in these two decades. From 1991 to 2000, the average frequency of heat waves began to rise, especially in the middle and west of Xinjiang province and the middle and lower reaches of the Jianghuai region. The number of heat waves in the Xinjiang region, Jianghuai region, and the middle and lower reaches of the Yangtze River increased significantly during 2001–2010 and 2011–2020, exceeding the average number of heat waves during 1961–1970. Combined with Figures 4 and 5b, the decadal variation trend in the duration of heat waves first decreased and then increased, which is basically consistent with the decadal variation trend of the frequency of heat waves. This result is consistent with the fact that the global climate is warming, glaciers are melting, and sea levels are rising.

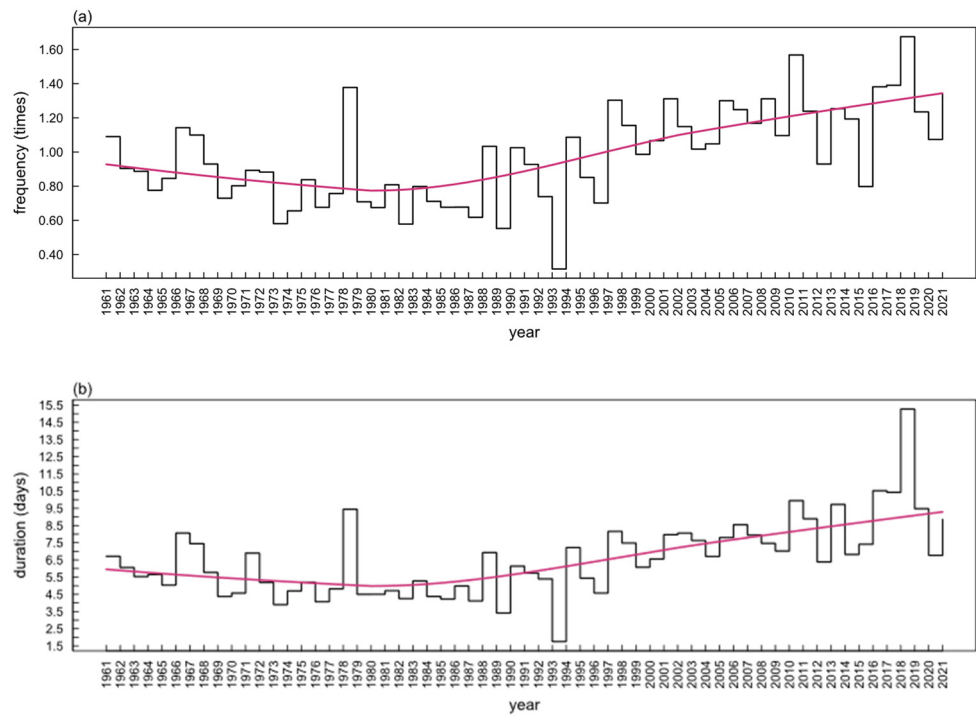


**Figure 5.** Based on the absolute method, the histogram of occurrence times and duration days of heat waves at each grid and the fitting line of the LOWESS trend were obtained. (a) Shows the average occurrence times of heat waves/number of grid points in each year from 1961 to 2021. (b) Shows the average number of days per grid point of heat waves in each year from 1961 to 2021.

(2) Earliest Date of Appearance and Latest Date of Extinction

According to the analysis of the earliest occurrence date and the latest extinction date of high-temperature heat waves obtained by the absolute method, the earliest occurrence time of heat waves was concentrated in June and July, and the latest extinction time was concentrated in August (Figure 6). The results obtained by the absolute method show that the occurrence and end of heat waves are concentrated in summer, which indicates that the absolute method can reasonably present the fact of hot and high temperatures in the summer for various regions.

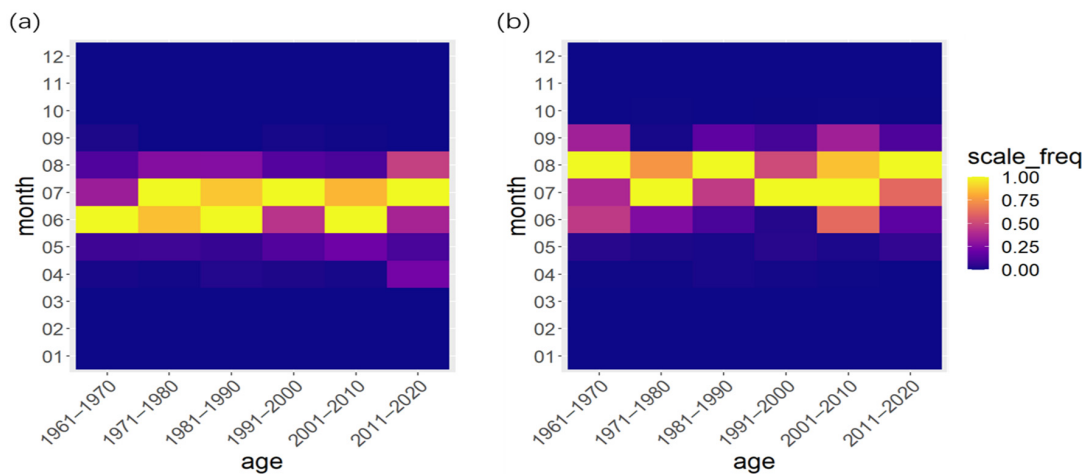


**Figure 6.** The distribution diagram of the earliest occurrence date and the latest extinction date of heat waves based on the absolute method. (a) Shows the distribution of the earliest occurrence date of heat waves in each month for each decade, and (b) Shows the distribution of the latest extinction date of heat waves in each month for each decade.

### 3.2.2. Results Based on Relative Methods

#### (1) Frequency and Intensity

Figure 7 depicts the decadal mean frequency distribution of heat waves screened using PTM (three consecutive days with maximum temperatures at least above the 90th percentile of the temperature series). Figure 8 depicts the corresponding average decadal duration of the selected heat waves. According to the results obtained by the relative method, almost all grid points have more than two times the amount of heat waves, and the duration of heat waves is more than 12 days, except for the Tibetan Plateau region in the 1960s. The average frequency and average duration of heat waves in the decadal period decreased first and then increased. The average frequency and average duration of decadal heat waves decreased from 1971 to 1980 and 1981 to 1990, began to rise from 1991 to 2000 and increased significantly from 2001 to 2010 and 2011 to 2020.

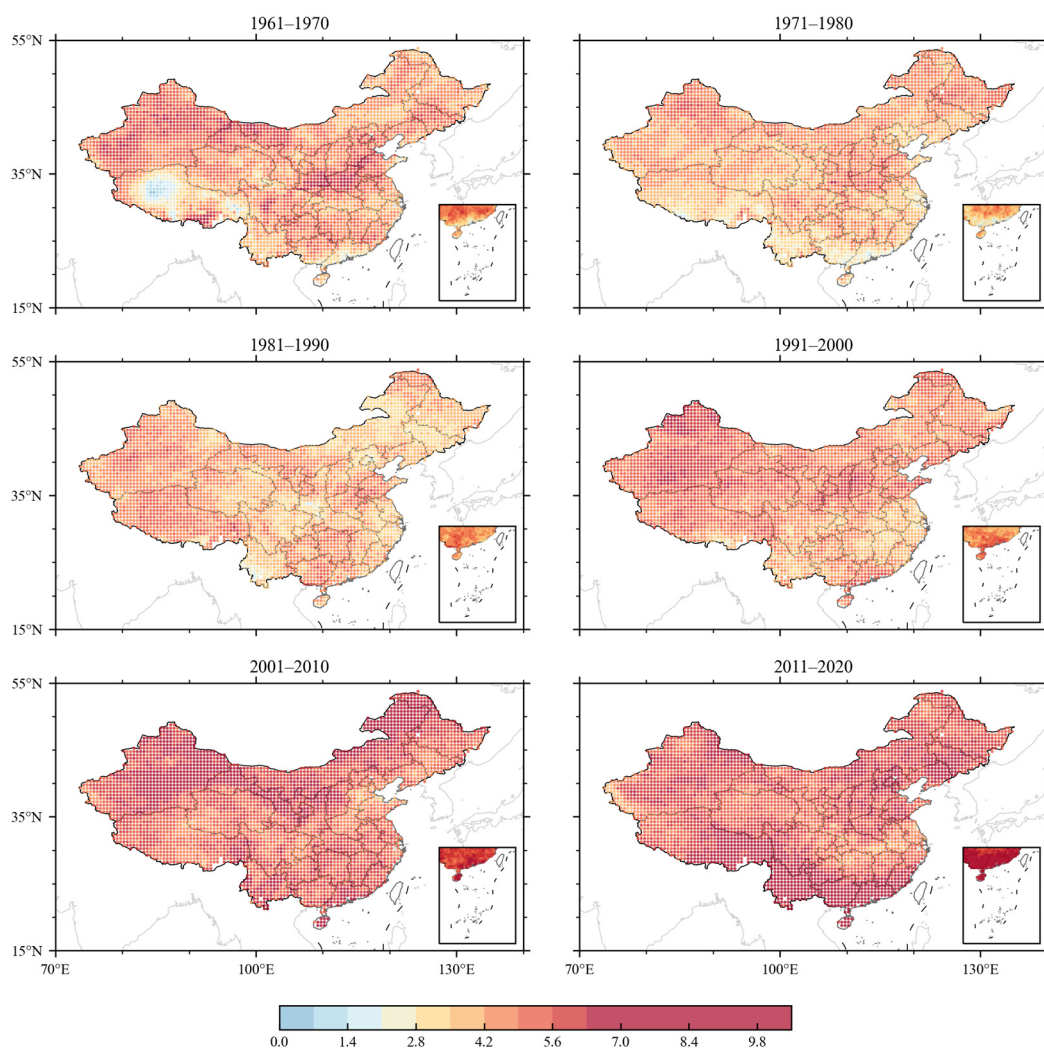


**Figure 7.** Distribution diagram of the decadal average frequency of heat waves based on PTM.

By comparing and analyzing Figures 3 and 7, we found that heat waves screened by the relative method were significantly more than those screened by the absolute method. China has a vast territory and huge terrain differences, and different regions have different fitness to temperature. The absolute method was used to unify high temperatures above 35 °C in different regions, and the relative method was used to define the high temperature in different regions as the 90th percentile of the temperature series in that region. The absolute method has high efficiency but ignores the tolerance degree of different regions to high temperatures. The relative method considers the different tolerance degrees of various

regions to high temperatures, but its efficiency is not as good as that of the relative method. The two methods have their own choice. Therefore, the absolute method and the relative method are used in this study to calculate heat waves. Some consistent results are obtained in the variation trend of the average frequency of high-temperature heat and the average duration of high-temperature heat in the decadal period. Regardless of the results of the absolute method or the relative method, the variation trend for the average occurrence times and average duration days of heat waves decreased from 1971 to 1980 and 1981 to 1990, began to rise from 1991 to 2000, and increased significantly from 2001 to 2010 and 2011 to 2020.

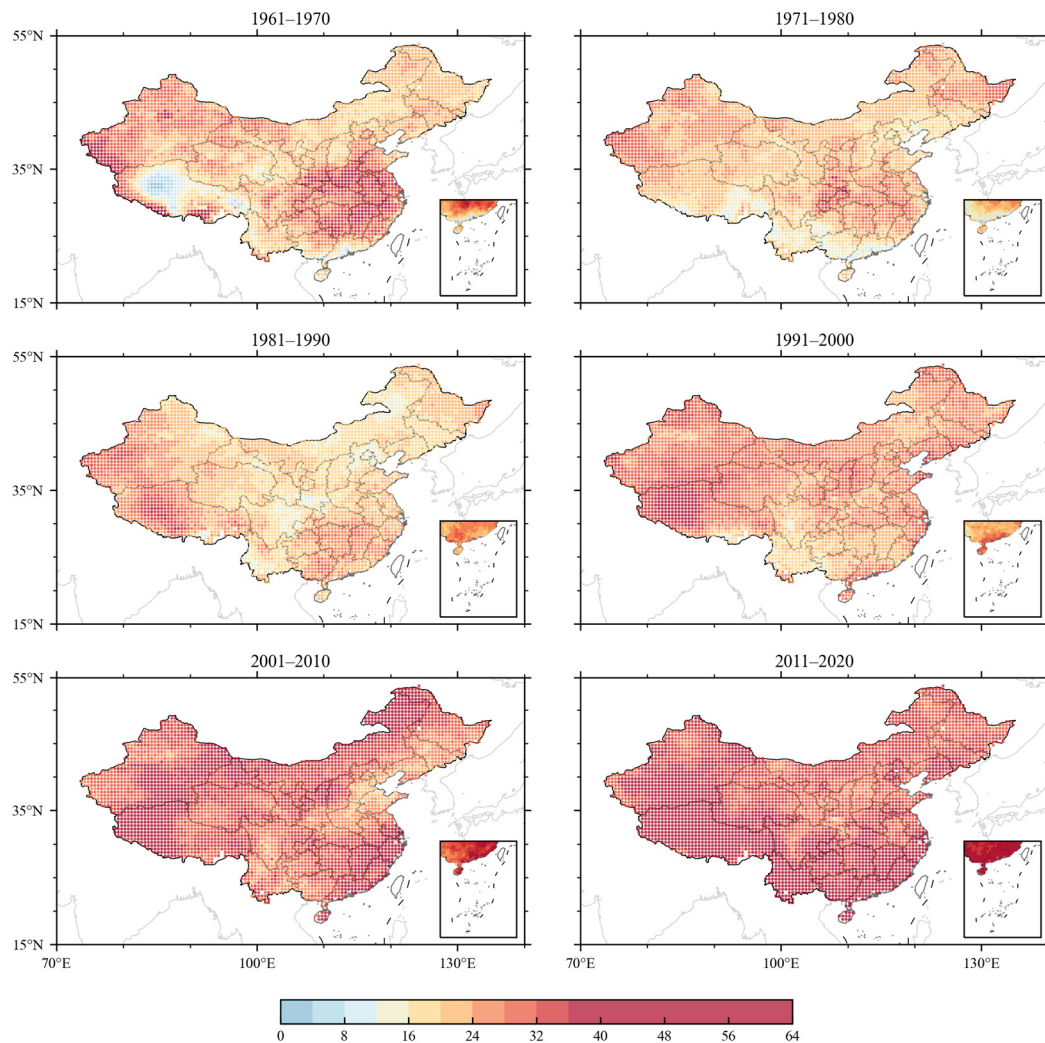


**Figure 8.** Distribution diagram of the decadal average duration days of heat waves based on PTM.

The decadal average occurrence times for the heat waves obtained are based on FATM (the anomaly of the maximum temperature on three consecutive days or more is not less than  $5^{\circ}\text{C}$ ), as shown in Figure 9. The characteristics of the decadal average frequency of heat waves screened by the standard of no less than  $5^{\circ}\text{C}$  show that the frequency of heat waves in eastern China and northern Xinjiang is more in space. The occurrence frequency was less in the central and southern regions of Xinjiang, Tibet, and Yunnan. Overall, there are more heat waves in the east and fewer heat waves in the west. The characteristics of the decadal average number of heat waves calculated by FATM showed a decrease in 1971–1980 and 1981–1990, a warming in 1991–2000, and a continuous increase in 2001–2010 and 2011–2020.

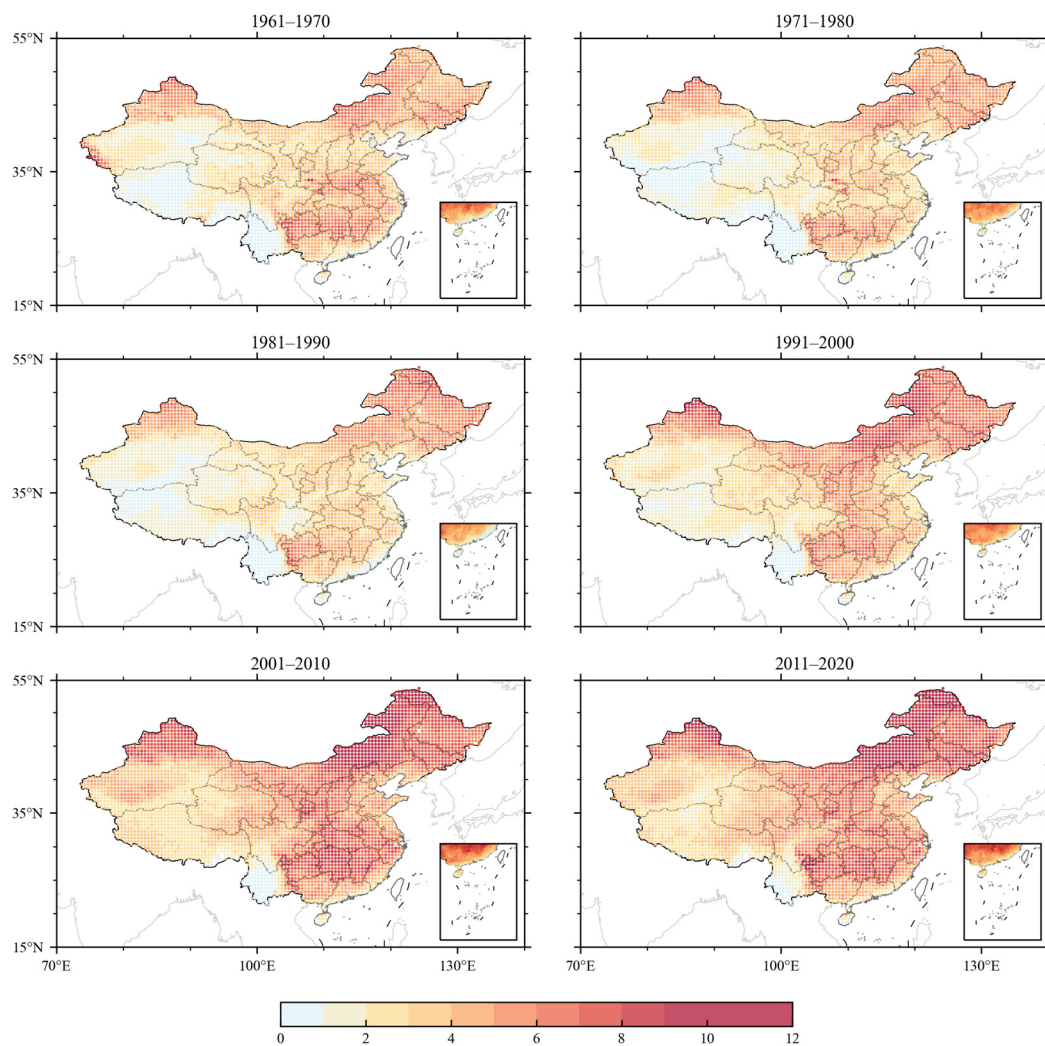


**Figure 9.** Distribution diagram of the decadal average frequency of heat waves based on FATM.

Based on FATM to screen out heat waves, the feature of decadal average duration days in space is that there are relatively more heat waves in the middle and lower reaches of the Yangtze River area, Inner Mongolia, and northern Xinjiang region. In terms of time, it shows the characteristics of decreasing first and then increasing significantly. These characteristics are similar to the results obtained by absolute and other relative methods as a whole (Figure 10).

Based on VATM (the daily maximum temperature anomaly of three consecutive days or more is no less than two times the standard deviation of the historical temperature series), the decadal average frequency of heat waves (Figure 11) is more spatial in western China but is not distinguished. It is also characterized by first decreasing and then increasing in time. The characteristics of the decadal average frequency of heat waves obtained by this relative method are very different from those obtained by other methods in space, but the characteristics of time are basically the same. The reason for the different spatial characteristics may be that VATM adopts standard deviation, which measures the degree of sequence dispersion. If the degree of sequence dispersion is large, the standard deviation is large; otherwise, the standard deviation is small. According to this standard, the heat waves in western China, especially in Tibet, can be explained. The annual temperature fluctuation in Tibet is relatively small, so the whole temperature series is relatively stable, and the standard deviation is small, so the anomaly can easily meet the screening condition of more than two times the standard deviation.

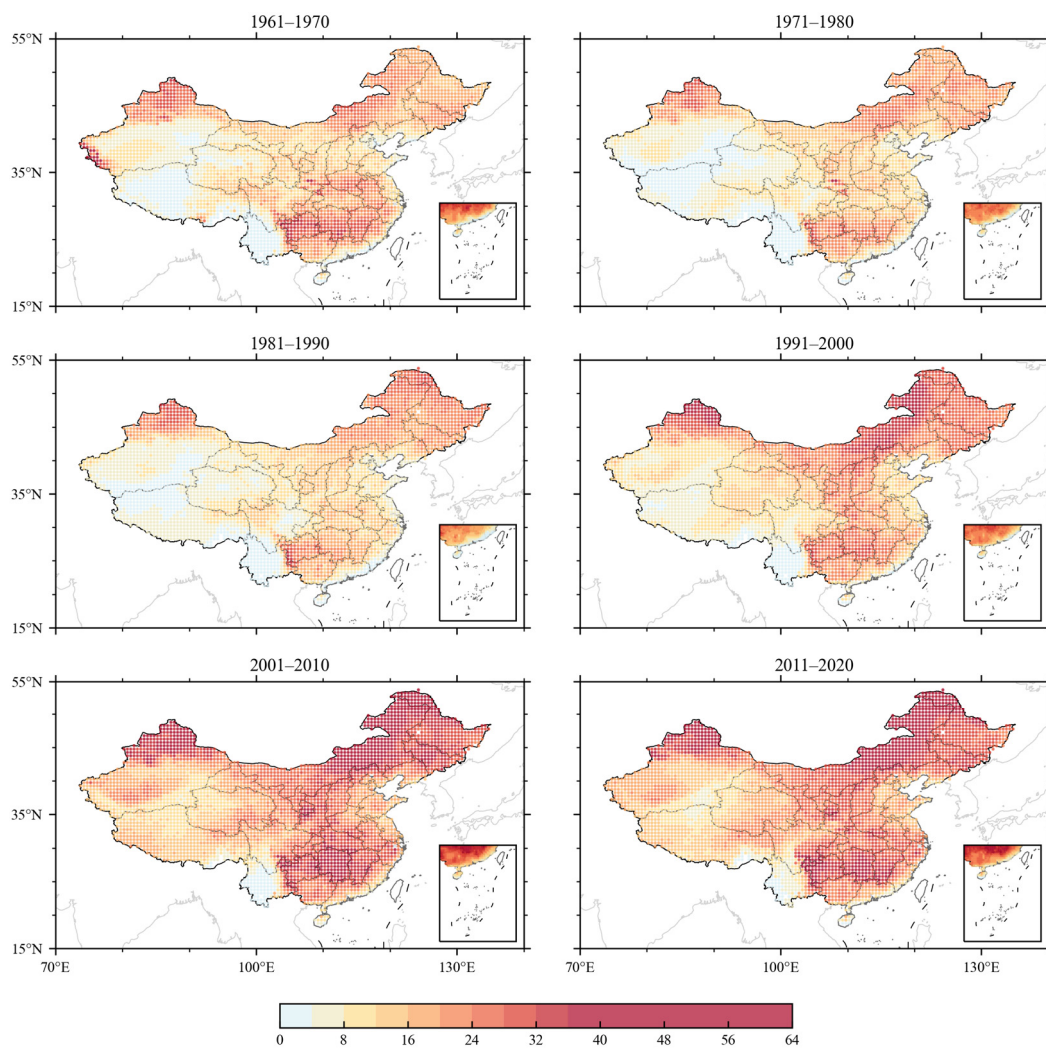


**Figure 10.** Distribution diagram of decadal average duration days of heat waves based on FATM.

The characteristics of decadal mean duration days of heat waves based on VATM (Figure 12) are more spatially situated in western China. The heat waves occurring in 1971–1980 and 1981–1990 were less than that during 1961–1970. During 1991–2000, it began to increase in the Tibet and Qinghai province. From 2001 to 2010 and from 2011 to 2020, the duration of heat waves in Xinjiang, eastern Inner Mongolia, the junction of Sichuan, Chongqing, and Guizhou, and the coastal areas of Jiangsu, Zhejiang, and Shanghai became longer.

According to PTM, the increase in heat waves on the decadal time scale is in central Tibet. According to FATM, heat waves increased in central and western China and the Jianghuai River basin on a decadal time scale. Using VATM, the regions with increased heat waves on the decadal time scale were the Tibetan plateau, eastern Inner Mongolia, and northern Xinjiang.

The difference between the absolute method and the relative method is that the absolute method had the same definition standard for high-temperature days in different regions, while the relative standard had inconsistent definition standards for high-temperature days in different regions, which led to the possibility of heat waves in any region based on the relative method. Therefore, the total number of heat waves and the total days obtained by the relative method were higher than those obtained by the absolute method. The three relative methods also had the different strictest screening conditions for heat waves. VATM had the strictest screening conditions for heat waves, followed by the second, and PTM had the loosest screening conditions. The severity degree corresponds to

the frequency and duration of high-temperature heat waves; that is, the more stringent the conditions, the weaker the frequency and intensity of heat waves, and the more relaxed the conditions, the stronger the frequency and intensity of heat waves.

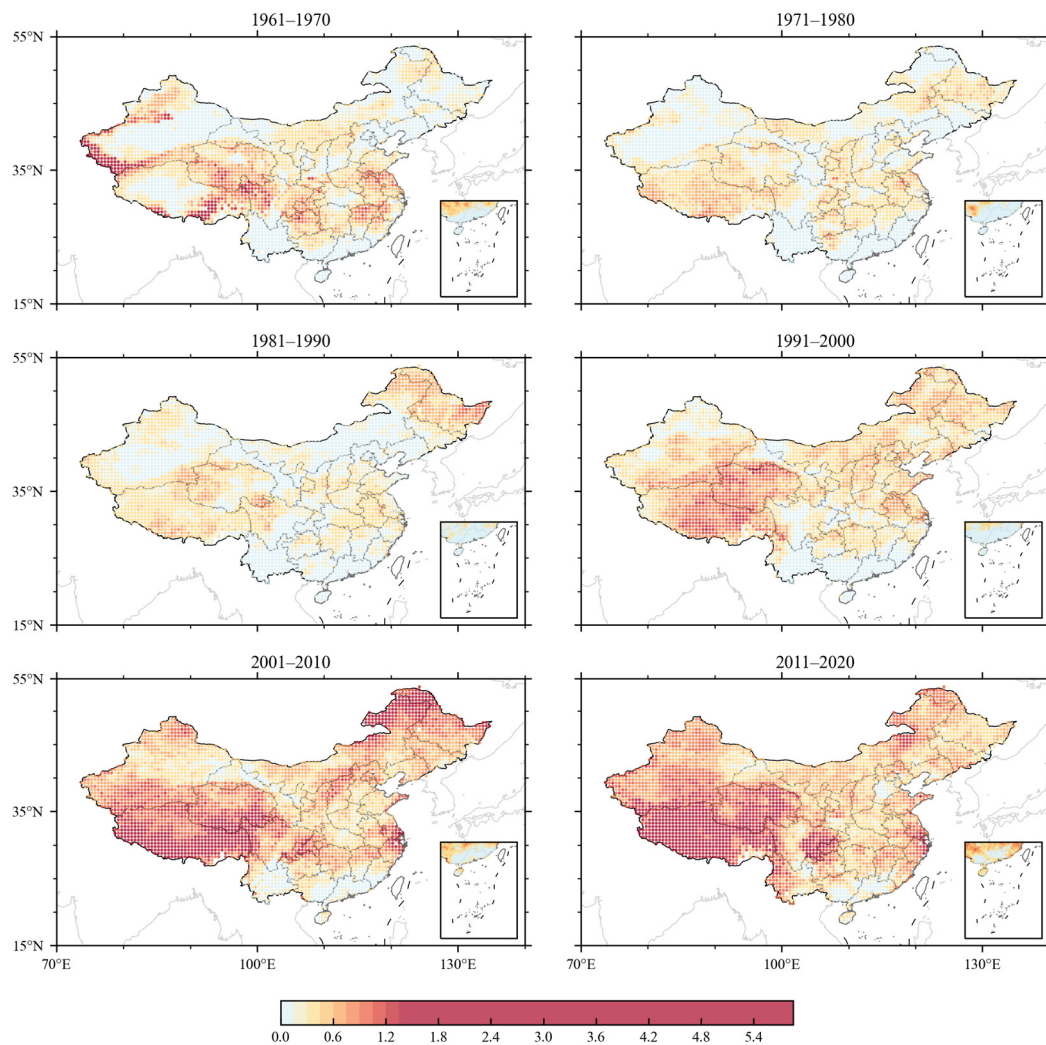


**Figure 11.** Distribution diagram of the decadal average frequency of heat waves based on VATM.

## (2) Earliest Date of Appearance and Latest Date of Extinction

According to PTM (90th percentile), the earliest occurrence date of the heat waves was concentrated in June, and the latest extinction date was concentrated in August, which is similar to the results obtained by the absolute method, and also proves that the 90th percentile threshold can capture the characteristics of summer high temperatures in each region (Figure 13). According to FATM (anomaly greater than five), the earliest occurrence date of heat waves mostly occurred in January, and the latest date of extinction was mostly in December. This result indicates that the sensitivity of each region to warming in winter is stronger than that in other seasons (Figure 13). According to VATM (anomaly greater than two times the standard deviation), the earliest date of occurrence for the heat waves accounted for a relatively high proportion in the first half of the year, while the latest date of extinction was relatively scattered. The extinction of heat waves occurred every month, and the earliest occurrence date showed a stepwise decline on the thermal map. The latest extinction date shows an upward trend bounded by the lower left and upper right diagonal line (Figure 13), which corresponds to the phenomenon that the occurrence time of heat waves is becoming earlier, and the extinction time is progressively later, which reflects the increase in the duration and intensity of heat waves.

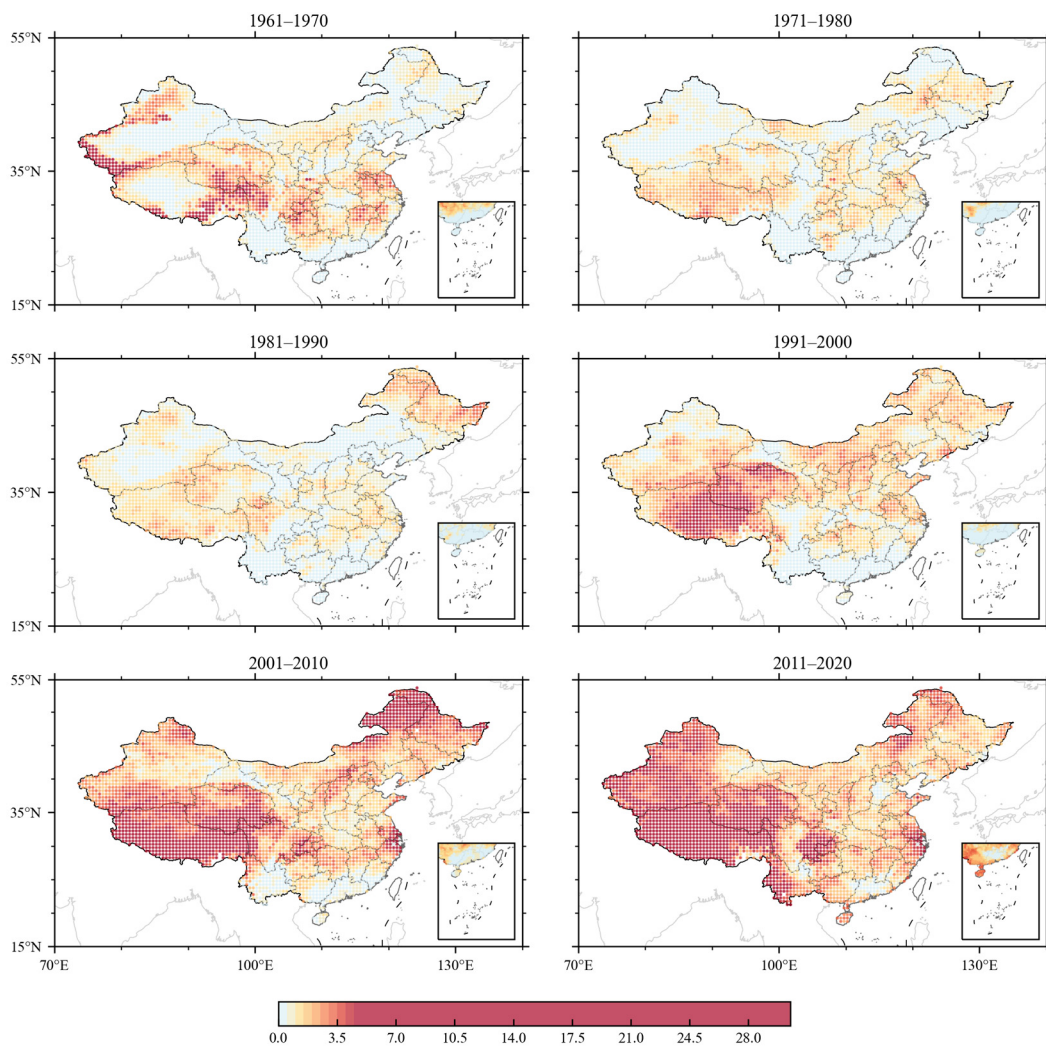


Figure 12. Distribution diagram of average days of heat waves in decades based on VATM.

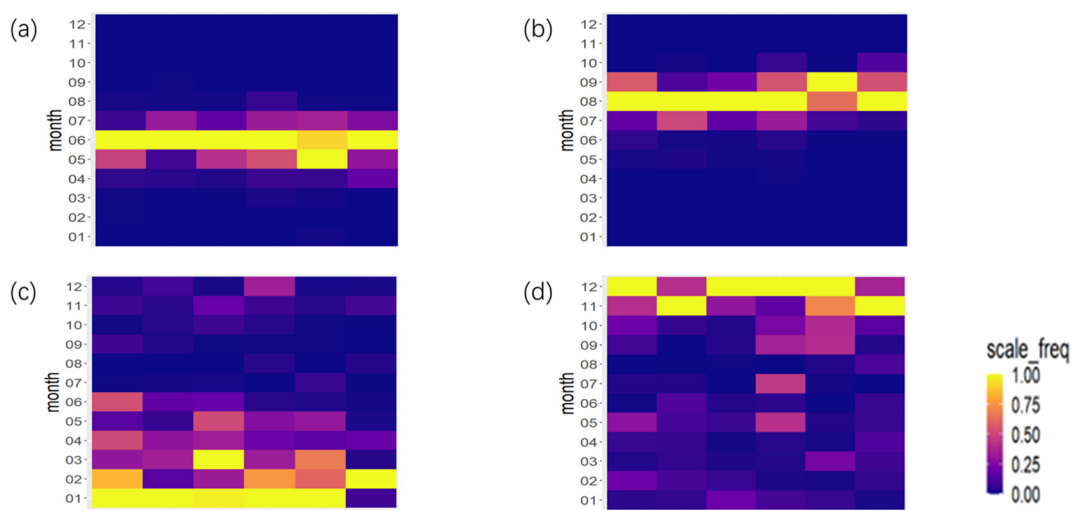
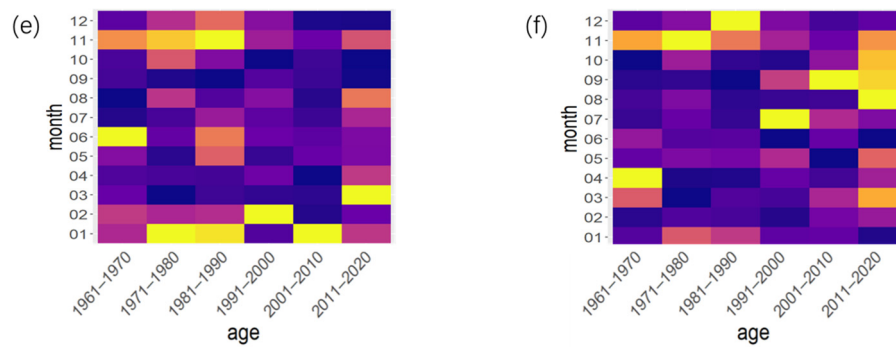


Figure 13. Cont.



**Figure 13.** The distribution of the earliest occurrence date and the latest extinction date of heat waves were obtained based on the relative method. (a) and (b), respectively, show the distribution of the earliest occurrence date and the latest extinction date of heat waves in each month obtained by PTM. (c) and (d), respectively, show the distribution of the earliest occurrence date and the latest extinction date of heat waves in each month obtained by FATM. (e) and (f), respectively, show the distribution of the earliest occurrence date and the latest extinction date of heat waves in each month obtained by VATM.

#### 4. Conclusions and Discussion

It is crucial to construct heat wave datasets from multiple angles, analyze the characteristics of heat waves, and derive their evolution characteristics to reduce the harm caused by heat waves to a certain extent. In this study, we used one absolute method and three relative methods to construct four heat wave datasets, counted four indicators of heat waves, and obtained the following spatiotemporal evolution characteristics of heat waves.

(1) During 1961–2020, the average daily maximum temperature in China remained stable from 1961–1980 and continued to rise from 1981 to 2020 with an obvious upward trend. The decadal average occurrence times and decadal average duration days of the heat waves obtained by the absolute and relative methods both decreased first and then increased [28,44,50]. Since the 1990s, the frequency and intensity of heat waves have increased significantly in response to global warming [26]. The first reason for this is the warming effect of the unusually strong subtropical high downdraft compression [28], and the second reason is that urbanization has been increasing since the 1990s [51]. Nonetheless, the regions of increasing heat waves obtained by different methods were not consistent. Based on the absolute method, we discovered that heat waves occurred most frequently both in the middle and lower reaches of the Yangtze river region and the Xinjiang region, which was consistent with the study by Ding et al. [28]. Based on three relative methods, we found that vast areas of China suffered from heat waves, which was also discussed by Li et al. [39] using a 35 °C threshold. These thresholds for measuring these heat waves are almost always at the tail end of the temperature distribution at any grid point on any calendar day. This conclusion shows that both absolute and relative methods can capture the evolution processes of heat waves well. The absolute method focuses on temperature itself, while relative methods focus on some other factors affecting temperature, which may be one of the reasons for the regional inconsistency of the heat waves increase.

(2) The earliest occurrence date and the latest extinction date of decadal heat waves obtained by the absolute method and relative methods are different as well. The possible reason for this is that different methods can give corresponding feedback to different heat wave characteristics. In this study, the causes of heat waves in different regions are not clear, and only preliminary inference is made through the similarities and differences of the evolution process of four statistical indicators of heat waves. The absolute method and PTM capture summer heat in various areas because of the characteristics of high temperatures. FATM captures the rule that regions are more sensitive to winter warming than other seasons. VATM captures the phenomenon of earlier onset and the later extinction of heat waves in China during 1961–2020.

In this study, an absolute method and three relative methods were used to screen heat waves, which was helpful in understanding the details of the characteristic changes in heat waves in mainland China [28]. Based on the absolute method and PTM, we captured the characteristics of heat waves that occurred more frequently in summer. Thus, we could strengthen summer heat wave monitoring and warnings to reduce the number of illnesses and deaths caused by heat waves. Based on FATM, we captured that the response to heat waves was greater in winter than in other seasons. Therefore, we could apply FATM statistical results to winter heat wave warnings. Based on VATM, we obtained results of increasing frequency and intensity of heat waves. Therefore, we call for urgent measures to slow the rate of global warming. Four kinds of thresholds could mark different features of heat waves as above, which might not be described by other researchers. Among the three relative methods selected in this study, FATM and VATM are rarely seen in other studies. Meanwhile, for the second and third relative methods, 365 was selected as the sampling interval to ensure that the temperature information of each calendar day was completely retained, which is different from other studies.

It is worth mentioning that abnormal atmospheric circulation is an important physical and meteorological cause of heat waves. The Western Pacific subtropical high is the main physical and meteorological cause of the heat wave in South China, the middle and lower reaches of the Yangtze River, and North China. The continuous and steady strengthening of the Western Pacific subtropical high is a favorable circulation situation to induce heat waves [52–54]. With a detailed understanding of the characteristics of heat waves, we will conduct further studies on physicometeorological causes based on snow cover and SST data.

The absolute threshold and PTM were used when we needed to monitor the high temperature defined by the thermometer. When we needed to monitor the somatosensory high temperature, we could utilize FATM and VATM. As mentioned in the introduction, heat waves affect mortality in summer [38,42]. Using the statistical tables of heat waves obtained by FATM and VATM, we may be able to further study the relationship between heat waves and mortality in winter so as to improve the heat wave warning mechanism. In addition, we can use different heat wave statistical data sets to provide diverse inputs for heat wave prediction models so as to fully learn the characteristics of heat waves and achieve accurate prediction. Different methods can provide a multi-dimensional reference for our next cause analysis and the prediction of heat waves.

**Author Contributions:** Conceptualization, A.F. (Aixia Feng) and C.G.; methodology, H.J., A.F. (Aiqing Feng); software, H.J.; validation, A.F. (Aixia Feng); formal analysis, H.J. and A.F. (Aixia Feng); investigation, A.F. (Aiqing Feng); resources and data curation, Y.Z. and J.L.; writing—original draft preparation, H.J.; writing—review and editing, A.F. (Aixia Feng) and C.G.; visualization, H.J. and Z.Z.; supervision, A.F. (Aixia Feng) and C.G. All authors have read and agreed to the published version of the manuscript.

**Funding:** This research was funded by the National Natural Science Foundation of China under grant Nos. 41975100, 12275179, 11875042 and 41905053, the Natural Science Foundation of Shanghai grant No. 21ZR1443900, and the China Meteorological Administration Special Foundations (grant number 22NLTZ004, CXFZ2022J050 and CXFZ2022J068).

**Institutional Review Board Statement:** Not applicable.

**Informed Consent Statement:** Not applicable.

**Data Availability Statement:** Not applicable.

**Acknowledgments:** We would like to thank our peers who volunteered to help with the experiment and the teachers who provided valuable comments on the article.

**Conflicts of Interest:** The authors declare no conflict of interest.

## References

1. Masson-Delmotte, V.; Zhai, P.; Pirani, A.; Connors, S.L.; Péan, C.; Berger, S.; Caud, N.; Chen, Y.; Goldfarb, L.; Gomis, M.I.; et al. IPCC, 2021: Summary for Policymakers. In *Climate Change 2021: The Physical Science Basis. Contribution of Working Group I to the Sixth Assessment Report of the Intergovernmental Panel on Climate Change*; Cambridge University Press: Cambridge, UK; New York, NY, USA, 2021; pp. 3–32.
2. Erdenebat, E.; Sato, T. Recent increase in heat wave frequency around Mongolia: Role of atmospheric forcing and possible influence of soil moisture deficit. *Atmos. Sci. Lett.* **2016**, *17*, 135–140. [[CrossRef](#)]
3. Perkins, S.E.; Alexander, L.V.; Nairn, J.R. Increasing frequency, intensity and duration of observed global heatwaves and warm spells. *Geophys. Res. Lett.* **2012**, *39*, 10. [[CrossRef](#)]
4. Mora, C.; Dousset, B.; Caldwell, I.R.; Powell, F.E.; Geronimo, R.C.; Coral, R.B.; Counsell, C.W.W.; Dietrich, B.S.; Johnston, E.T.; Louis, L.V.; et al. Global risk of deadly heat. *Nat. Clim. Chang.* **2017**, *7*, 501–506. [[CrossRef](#)]
5. Russo, S.; Sillmann, J.; Sterl, A. Humid heat waves at different warming levels. *Sci. Rep.* **2017**, *7*, 7477. [[CrossRef](#)]
6. Sun, Y.; Zhang, X.; Zwiers, F.W.; Song, L.; Wan, H.; Hu, T.; Yin, H.; Ren, G. Rapid increase in the risk of extreme summer heat in Eastern China. *Nat. Clim. Chang.* **2014**, *4*, 1082–1085. [[CrossRef](#)]
7. Wang, Y.; Zhou, B.; Qin, D.; Wu, J.; Gao, R.; Song, L. Changes in mean and extreme temperature and precipitation over the arid region of northwestern China: Observation and projection. *Adv. Atmos. Sci.* **2017**, *34*, 289–305. [[CrossRef](#)]
8. Wang, W.; Zhou, W.; Li, Y.; Wang, X.; Wang, D. Statistical modeling and CMIP5 simulations of hot spell changes in China. *Clim. Dyn.* **2014**, *44*, 2859–2872. [[CrossRef](#)]
9. Robine, J.M.; Cheung, S.L.; Le Roy, S.; Van Oyen, H.; Griffiths, C.; Michel, J.P.; Herrmann, F.R. Death toll exceeded 70,000 in Europe during the summer of 2003. *Comptes Rendus Biol.* **2008**, *331*, 171–178. [[CrossRef](#)]
10. Trigo, R.M.; Ramos, A.M.; Nogueira, P.J.; Santos, F.D.; Garcia-Herrera, R.; Gouveia, C.; Santo, F.E. Evaluating the impact of extreme temperature based indices in the 2003 heatwave excessive mortality in Portugal. *Environ. Sci. Policy* **2009**, *12*, 844–854. [[CrossRef](#)]
11. Barriopedro, D.; Fischer, E.M.; Luterbacher, J.; Trigo, R.M.; García-Herrera, R. The hot summer of 2010: Redrawing the temperature record map of Europe. *Science* **2011**, *332*, 220–224. [[CrossRef](#)]
12. Katsafados, P.; Papadopoulos, A.; Varlas, G.; Papadopoulou, E.; Mavromatidis, E. Seasonal predictability of the 2010 Russian heat wave. *Nat. Hazards Earth Syst. Sci.* **2014**, *14*, 1531–1542. [[CrossRef](#)]
13. Quandt, L.-A.; Keller, J.H.; Martius, O.; Jones, S.C. Forecast Variability of the Blocking System over Russia in Summer 2010 and Its Impact on Surface Conditions. *Weather Forecast.* **2017**, *32*, 61–82. [[CrossRef](#)]
14. Xia, J.; Tu, K.; Yan, Z.; Qi, Y. The super-heat wave in eastern China during July–August 2013: A perspective of climate change. *Int. J. Climatol.* **2016**, *36*, 1291–1298. [[CrossRef](#)]
15. Sánchez-Benítez, A.; García-Herrera, R.; Barriopedro, D.; Sousa, P.M.; Trigo, R.M. June 2017: The Earliest European Summer Mega-heatwave of Reanalysis Period. *Geophys. Res. Lett.* **2018**, *45*, 1955–1962. [[CrossRef](#)]
16. Ahn, K.H. Interannual variability of heat waves over the Korean Peninsula based on integrated approach. *Sci. Total Environ.* **2022**, *826*, 154153. [[CrossRef](#)]
17. Baldwin, J.W.; Dessy, J.B.; Vecchi, G.A.; Oppenheimer, M. Temporally Compound Heat Wave Events and Global Warming: An Emerging Hazard. *Earth's Future* **2019**, *7*, 411–427. [[CrossRef](#)]
18. Cherchi, A.; Annamalai, H.; Masina, S.; Navarra, A. South Asian Summer Monsoon and the Eastern Mediterranean Climate: The Monsoon–Desert Mechanism in CMIP5 Simulations. *J. Clim.* **2014**, *27*, 6877–6903. [[CrossRef](#)]
19. Stanojevic, G.; Spalević, A.B.; Kokotović, V.M.; Stojilković, J.N. Does Belgrade (Serbia) need heat health warning system? *Disaster Prev. Manag.* **2014**, *23*, 494–507. [[CrossRef](#)]
20. Wang, J.; Feng, J.; Yan, Z.; Chen, Y. Future Risks of Unprecedented Compound Heat Waves over Three Vast Urban Agglomerations in China. *Earth's Future* **2020**, *8*, e2020EF001716. [[CrossRef](#)]
21. Schauburger, B.; Archontoulis, S.; Arneeth, A.; Balkovic, J.; Ciais, P.; Deryng, D.; Elliott, J.; Folberth, C.; Khabarov, N.; Muller, C.; et al. Consistent negative response of US crops to high temperatures in observations and crop models. *Nat. Commun.* **2017**, *8*, 13931. [[CrossRef](#)]
22. Ban, J.; Xu, D.; He, M.Z.; Sun, Q.; Chen, C.; Wang, W.; Zhu, P.; Li, T. The effect of high temperature on cause-specific mortality: A multi-county analysis in China. *Environ. Int.* **2017**, *106*, 19–26. [[CrossRef](#)]
23. Moraes, S.L.; Almendra, R.; Barrozo, L.V. Impact of heat waves and cold spells on cause-specific mortality in the city of Sao Paulo, Brazil. *Int. J. Hyg. Environ. Health* **2022**, *239*, 113861. [[CrossRef](#)]
24. Russo, S.; Dosio, A.; Graversen, R.G.; Sillmann, J.; Carrao, H.; Dunbar, M.B.; Singleton, A.; Montagna, P.; Barbola, P.; Vogt, J.V. Magnitude of extreme heat waves in present climate and their projection in a warming world. *J. Geophys. Res. Atmos.* **2014**, *119*, 12500–12512. [[CrossRef](#)]
25. Guo, X.; Huang, J.; Luo, Y.; Zhao, Z.; Xu, Y. Projection of heat waves over China for eight different global warming targets using 12 CMIP5 models. *Theor. Appl. Climatol.* **2016**, *128*, 507–522. [[CrossRef](#)]
26. Sun, Y.; Hu, T.; Zhang, X. Substantial Increase in Heat Wave Risks in China in a Future Warmer World. *Earth's Future* **2018**, *6*, 1528–1538. [[CrossRef](#)]
27. Wang, P.; Hui, P.; Xue, D.; Tang, J. Future projection of heat waves over China under global warming within the CORDEX-EA-II project. *Clim. Dyn.* **2019**, *53*, 957–973. [[CrossRef](#)]

28. Ding, T.; Qian, W.; Yan, Z. Changes in hot days and heat waves in China during 1961–2007. *Int. J. Climatol.* **2010**, *30*, 1452–1462. [[CrossRef](#)]
29. Perkins-Kirkpatrick, S.E.; Lewis, S.C. Increasing trends in regional heatwaves. *Nat. Commun.* **2020**, *11*, 3357. [[CrossRef](#)]
30. Tong, S.; Wang, X.Y.; FitzGerald, G.; McRae, D.; Neville, G.; Tippet, V.; Aitken, P.; Verrall, K. Development of health risk-based metrics for defining a heatwave: A time series study in Brisbane, Australia. *BMC Public Health* **2014**, *14*, 435. [[CrossRef](#)]
31. Bador, M.; Terray, L.; Boe, J.; Somot, S.; Alias, A.; Gibelin, A.-L.; Dubuisson, B. Future summer mega-heatwave and record-breaking temperatures in a warmer France climate. *Environ. Res. Lett.* **2017**, *12*, 074025. [[CrossRef](#)]
32. Chen, Y.; Li, Y. An Inter-comparison of Three Heat Wave Types in China during 1961–2010: Observed Basic Features and Linear Trends. *Sci. Rep.* **2017**, *7*, 45619. [[CrossRef](#)]
33. Chen, R.; Wen, Z.; Lu, R. Evolution of the Circulation Anomalies and the Quasi-Biweekly Oscillations Associated with Extreme Heat Events in Southern China. *J. Clim.* **2016**, *29*, 6909–6921. [[CrossRef](#)]
34. Tan, J.; Huang, J. The Impacts of Heat Waves on Human Health and Its Research Methods. *Clim. Environ. Res.* **2004**, *9*, 680–686.
35. Huynen, M.-M.; Martens, P.; Schram, D.; Weijenberg, M.P.; Kunst, A.E. The impact of heat waves and cold spells on mortality rates in the Dutch population. *Environ. Health Perspect.* **2001**, *109*, 463–470. [[CrossRef](#)]
36. Pan, Y.Z.; Wang, J.A.; Gong, D.Y. Changes in extreme daily mean temperatures in summer in eastern China during 1955–2000. *Theor. Appl. Climatol.* **2004**, *77*, 25–37. [[CrossRef](#)]
37. Shi, J.; Tang, X.; Cui, L. Climatic characteristics of high temperature in East China during 1961–2005. *J. Geogr. Sci.* **2008**, *18*, 283–294. [[CrossRef](#)]
38. Tan, J.; Zheng, Y.; Song, G.; Kalkstein, L.S.; Kalkstein, A.J.; Tang, X. Heat wave impacts on mortality in Shanghai, 1998 and 2003. *Int. J. Biometeorol.* **2007**, *51*, 193–200. [[CrossRef](#)]
39. Li, K.; Amatus, G. Spatiotemporal changes of heat waves and extreme temperatures in the main cities of China from 1955 to 2014. *Nat. Hazards Earth Syst. Sci.* **2020**, *20*, 1889–1901. [[CrossRef](#)]
40. Purich, A.; Cowan, T.; Perkins, S.; Pezza, A.; Boschat, G.; Sadler, K. More Frequent, Longer, and Hotter Heat Waves for Australia in the Twenty-First Century. *J. Clim.* **2014**, *27*, 5851–5871. [[CrossRef](#)]
41. Ding, T.; Qian, W. Geographical patterns and temporal variations of regional dry and wet heatwave events in China during 1960–2008. *Adv. Atmos. Sci.* **2011**, *28*, 322–337. [[CrossRef](#)]
42. Zimmer, J.; Tong, S.; Wang, X.Y.; Barnett, A.G. Assessment of Heat-Related Health Impacts in Brisbane, Australia: Comparison of Different Heatwave Definitions. *PLoS ONE* **2010**, *5*, e12155. [[CrossRef](#)]
43. Zhou, Y.; Ren, G. Change in extreme temperature event frequency over mainland China, 1961–2008. *Clim. Res.* **2011**, *50*, 125–139. [[CrossRef](#)]
44. Ding, T.; Ke, Z. Characteristics and changes of regional wet and dry heat wave events in China during 1960–2013. *Theor. Appl. Climatol.* **2014**, *122*, 651–665. [[CrossRef](#)]
45. Wang, P.; Tang, J.; Sun, X.; Wang, S.; Wu, J.; Dong, X.; Fang, J. Heat Waves in China: Definitions, Leading Patterns, and Connections to Large-Scale Atmospheric Circulation and SSTs. *J. Geophys. Res. Atmos.* **2017**, *122*, 10679–10699. [[CrossRef](#)]
46. You, Q.; Jiang, Z.; Kong, L.; Wu, Z.; Bao, Y.; Kang, S.; Pepin, N. A comparison of heat wave climatologies and trends in China based on multiple definitions. *Clim. Dyn.* **2016**, *48*, 3975–3989. [[CrossRef](#)]
47. Wang, J.; Yan, Z. Rapid rises in the magnitude and risk of extreme regional heat wave events in China. *Weather. Clim. Extrem.* **2021**, *34*, 100379. [[CrossRef](#)]
48. Perkins, S.E. A review on the scientific understanding of heatwaves—Their measurement, driving mechanisms, and changes at the global scale. *Atmos. Res.* **2015**, *164–165*, 242–267. [[CrossRef](#)]
49. Cleveland, W.S. Robust Locally Weighted Regression and Smoothing Scatterplots. *J. Am. Stat. Assoc.* **1979**, *74*, 829–836. [[CrossRef](#)]
50. Wang, P.; Tang, J.; Wang, S.; Dong, X.; Fang, J. Regional heatwaves in China: A cluster analysis. *Clim. Dyn.* **2017**, *50*, 1901–1917. [[CrossRef](#)]
51. Kong, D.; Gu, X.; Li, J.; Ren, G.; Liu, J. Contributions of Global Warming and Urbanization to the Intensification of Human-Perceived Heatwaves Over China. *J. Geophys. Res. Atmos.* **2020**, *125*, e2019JD032175. [[CrossRef](#)]
52. Liu, Q.; Zhou, T.; Mao, H.; Fu, C. Decadal Variations in the Relationship between the Western Pacific Subtropical High and Summer Heat Waves in East China. *J. Clim.* **2019**, *32*, 1627–1640. [[CrossRef](#)]
53. Li, J.; Ding, T.; Jia, X.; Zhao, X. Analysis on the Extreme Heat Wave over China around Yangtze River Region in the Summer of 2013 and Its Main Contributing Factors. *Adv. Meteorol.* **2015**, *2015*, 706713. [[CrossRef](#)]
54. Wang, W.; Zhou, W.; Li, X.; Wang, X.; Wang, D. Synoptic-scale characteristics and atmospheric controls of summer heat waves in China. *Clim. Dyn.* **2015**, *46*, 2923–2941. [[CrossRef](#)]

**Disclaimer/Publisher’s Note:** The statements, opinions and data contained in all publications are solely those of the individual author(s) and contributor(s) and not of MDPI and/or the editor(s). MDPI and/or the editor(s) disclaim responsibility for any injury to people or property resulting from any ideas, methods, instructions or products referred to in the content.